Optical Magnetometry

Principles and presentation of a magnetometer operating in unshielded environment

Giuseppe Bevilacqua, Valerio Biancalana, Yordanka Dancheva, Antonio Vigilante

UNIVERSITÀ
DI SIENA
1240

Abstract

Optical Magnetometry can be exploited to perform high sensitivity measurements using low cost experimental apparatus. Despite this research field is active since a long time –first theoretical and experimental studies started in 1960s– nowadays it finds a renewed interest, also thanks to advances in laser technology and numerical data elaboration.
The multiplicity of configurations available to perform magnetic measurements using atoms opens to various applications in field such as fundamental physics, nuclear magnetic resonance, geophysics, security and environment.
The talk is divided in two main parts. The first is about the principles of optical magnetometry focusing on most used set-up. The latter presents more specifically the unshielded optical magnetometer developed in our laboratory; focusing on our efforts to increase instrumental sensitivity and to attempt magnetic resonance imaging measurements.

General Principle

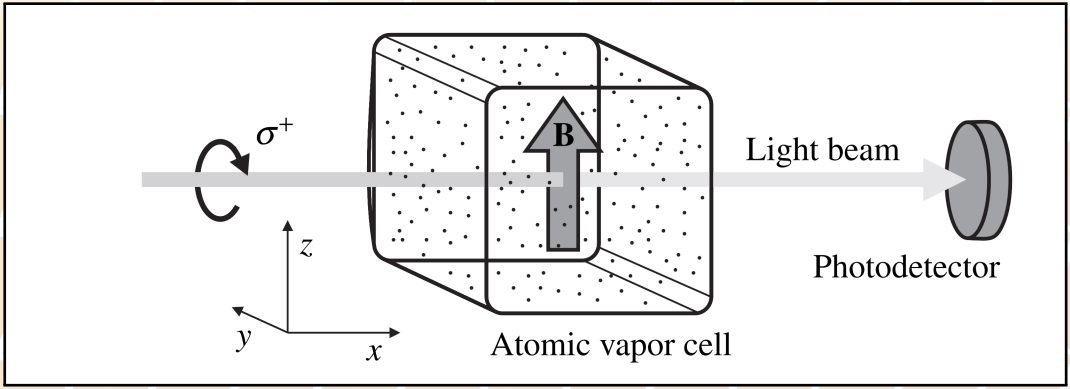

Polarization by Optical Pumping (1)

The transfer of order from a light beam to an atomic vapour takes place as a result of two different mechanisms, depopulation pumping and repopulation pumping.

- Depopulation pumping occurs when certain ground state sublevels absorb light more strongly than others. Since atoms are removed more rapidly from the strongly absorbing sublevels, an excess population will tend to build up in the weakly absorbing sublevels.

W. HAPPER, "Optical pumping," *Rev. Mod. Phys.*, vol. 44, pp. 169–249, Apr 1972

Polarization by Optical Pumping (2)

The optical pumping technique described is depopulation pumping with circularly polarized light; other kinds of magnetometers (as well as other applications such as atomic clocks) may use different techniques.

- $\sigma+$ polarized light
- $\hat{z}$ the direction of propagation of the beam
- $C, m_J = -1/2 \rightarrow E, m_J = +1/2$

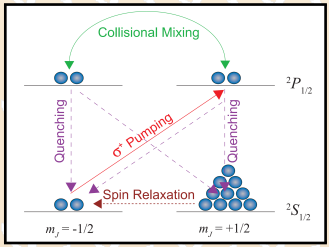

S. J. Seltzer, *Developments in alkali-metal atomic magnetometry*. Princeton University, 2008

Polarization by Optical Pumping (2)

The optical pumping technique described is depopulation pumping with circularly polarized light; other kinds of magnetometers (as well as other applications such as atomic clocks) may use different techniques.

A chemically inert buffer gas used to prevent wall collisions (spin relaxation).
Collisions with buffer gas atoms depolarize the alkali atoms causing a collisional mixing between the Zeeman levels of the excited state (larger cross section) that equalizes the populations of the levels.

Atoms spontaneously decay back to the ground state emitting a randomly polarized resonant photon that can depolarize another atom if reabsorbed.
To prevent such a quenching gas (such as N2) is added. Atoms transfer their excess energy to the rotational and vibrational modes of the quenching gas molecules and decay back to the ground state without radiating a resonant photon.

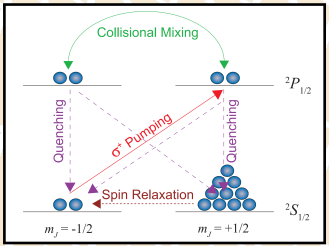

S. J. Seltzer, *Developments in alkali-metal atomic magnetometry*. Princeton University, 2008

Polarization by Optical Pumping (3)

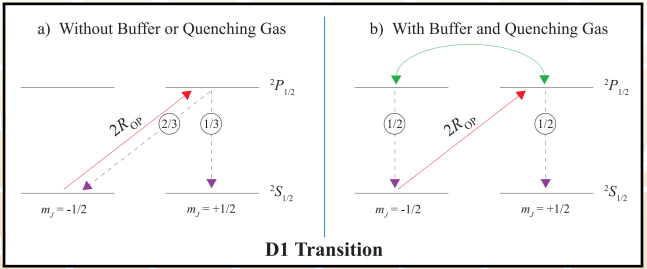

Collisional mixing makes the optical pumping process more efficient since the atoms have a greater probability of decaying to the $m_J = +1/2$ sublevel. With an adequate collisional mixing rate equations are:

$$\frac{d}{dt}\rho(-1/2) = -2R_{OP}\rho(-1/2) + \frac{1}{2}2R_{OP}\rho(-1/2)$$

$$\frac{d}{dt}\rho(+1/2) = +\frac{1}{2}2R_{OP}\rho(-1/2)$$

$$\langle S_z \rangle = \frac{1}{2}\left[\rho(+1/2) - \rho(-1/2)\right] = \frac{1}{2}\left(1 - e^{-R_{OP}t}\right)$$

S. J. Seltzer, *Developments in alkali-metal atomic magnetometry*. Princeton University, 2008

Polarization by Optical Pumping (4)

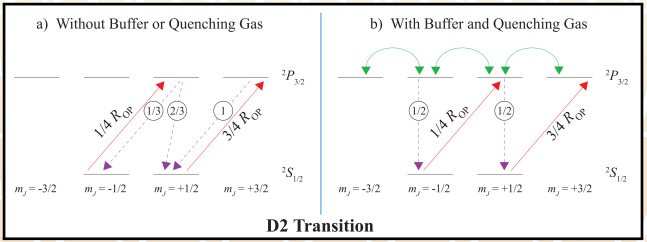

$$\langle S_z \rangle = \frac{1}{2}\left[\rho(+1/2) - \rho(-1/2)\right] = \frac{1}{4}\left(e^{-R_{OP}t} - 1\right)$$

The spin polarization in this case is only half of its value in the case of D1 pumping, limiting the maximum polarization.

S. J. Seltzer, *Developments in alkali-metal atomic magnetometry*. Princeton University, 2008

Atom Field Interaction

For polarized atoms with ground state angular momentum F, the atom-field interaction strength is characterized by the Larmor frequency

$$\omega_L = \frac{g_F \mu_B}{\hbar} |\boldsymbol{B}_0| = \gamma_F |\boldsymbol{B}_0|$$

The power of magnetic resonance-based magnetometers lies in the fact that they allow for a direct measurement of the Larmor frequency, and hence of the magnetic field, with an accuracy, that is, in principle, only limited by the accuracy with which the gyromagnetic ratio γ_F is known.

Optical Detection(1)

The magnetic field induced alterations of the spin polarization alter the optical properties of the atomic medium, the latter affecting themselves the properties of a probe light beam traversing the atomic medium. The magnetometric information may thus be extracted from either:

- The power of the probe beam traversing the medium,
- The polarization of the probe beam traversing the medium,
- The intensity of fluorescence induced by the probe beam[1],
- The power (polarization) of retro-reflected probe beam[2] .

[1] I. Fescenko and A. Weis, "Imaging magnetic scalar potentials by laser-induced fluorescence from bright and dark atoms," *Journal of Physics D: Applied Physics*, vol. 47, p. 235001, may 2014

[2] A. Weis, V. A. Sautenkov, and T. W. Hänsch, "Observation of ground-state zeeman coherences in the selective reflection from cesium vapor," *Phys. Rev. A*, vol. 45, pp. 7991–7996, Jun 1992

Optical Detection(2)

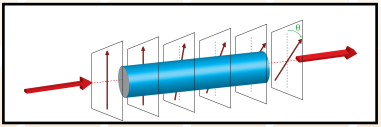

A signal detection techniques use the optical rotation of an off-resonant, linearly polarized probe beam. The probe beam propagates along a direction i. Its plane of polarization rotates by an angle $\theta \propto \langle S_i \rangle$ due to a difference in the indices of refraction $n_+(\nu)$ and $n_-(\nu)$ experienced by σ_+ and σ_- light, respectively.

$$\theta = \frac{\pi \nu l}{c} [n_+(\nu) - n_-(\nu)]$$

For resonant light interaction the process is named as Macaluso Corbino Effect.

$$n_-(\nu) = 1 + 2\left(\frac{3}{4}\rho(-1/2) + \frac{1}{4}\rho(+1/2)\right)\left(\frac{n r_e c^2 f_{D2}}{4\nu}\right) Im[\mathcal{L}(\nu - \nu_{D2})]$$

$$n_+(\nu) = 1 + 2\left(\frac{1}{4}\rho(-1/2) + \frac{3}{4}\rho(+1/2)\right)\left(\frac{n r_e c^2 f_{D2}}{4\nu}\right) Im[\mathcal{L}(\nu - \nu_{D2})]$$

Thus, the atomic vapor is birefringent when $\rho(-1/2) \neq \rho(+1/2)$

Fundamental Sensitivity

The spin-projection-noise-limited (or atomic shot-noise-limited) sensitivity δB_{SNL} of a polarized atomic sample to magnetic fields is determined by the total number of atoms N and the spin-relaxation rate Γ_{rel} for measurement times $\tau >> \Gamma_{rel}^{-1}$

$$\delta B_{SNL} \approx \frac{1}{\gamma}\sqrt{\frac{\Gamma_{rel}}{N\tau}}$$

Defining $\Gamma_{rel} = \xi n$ with ξ ranging between $\sim 10^{-9} cm^3/s$ and $\sim 10^{-13} cm^3/s$

$$\delta B_{SNL} \approx \frac{1}{\gamma}\sqrt{\frac{\xi}{V\tau}}$$

Thus for optical magnetometers using alkali vapours, the optimal magnetometric sensitivity for a $V = 1cm^3$ magnetic sensor ranges between 10^{11} and 10^{13} G/$\sqrt{Hz}$ (1 to 0.01 fT/$\sqrt{Hz}$).

Optical Magnetometry. Cambridge University Press, 2013

There is no best magnetometer, but there is a best suited magnetometer for every application

- Sensitivity (ability to detect field changes) is only one characteristic property of a given magnetometer.
- Accuracy (ability to infer the absolute field value), e.g., is a property that has not been given much attention in the atomic magnetometers community.
- How does the magnetometer's sensitivity compare to its accuracy?
- Does it measure quasi-static or oscillating fields?
- For what range of field strengths can it be used (dynamic range)?
- How fast does it react to a sudden field change (measurement bandwidth)?
- Can it be turned into a portable device?
- Is it meant to monitor a laboratory field whose magnitude and orientation are known a priori?
- Which field direction maximizes its sensitivity, what are its orientational dead zones?
- Does the device suffer from heading errors, i.e., are its field readings dependent on the field orientation?
- Does the method allow the easy deployment of the device in a multi-sensor array?
- Can the magnetometer be operated in harsh (vacuum, airborne, space-borne, underwater) conditions?
- Does the device's stability allow long-time (hours/days) measurements?

Vector and Scalar Magnetometers

- Vector magnetometers can measure all three components of the magnetic field and thus can obtain more complete information about the field and provide much better localization information for detection of magnetic-anomaly sources. On the other hand, vector magnetometers are much more sensitive to rotations. Therefore, vector magnetometers have to be mounted on stationary platforms, combined with sensitive gyroscopes, or used in combination to form magnetic gradiometers.
- Scalar magnetometers are insensitive to rotation of the magnetometer in the Earth's magnetic field and rely on frequency measurements which can be made with very high accuracy. Since the relation between the frequency and the magnetic field depends only on fundamental constants.
  Note that a scalar magnetometer, when operated in a an offset field $|\mathbf{B}_0| = B_0 \hat{\mathbf{z}}$ can be used to detect a single vector component of a much weaker field $\delta\mathbf{B}$ with components $(\delta B_x, \delta B_y, \delta B_z)$. Since the magnetometer measures the field modulus, one has:

$$B_{tot} = |\mathbf{B}_{tot}| = |\mathbf{B}_0 + \delta\mathbf{B}| \approx B_0 + \delta B_z + \mathcal{O}(\delta B_i^2)$$

  so that the magnetometer detects effectively only one vector component.

Optical magnetometers are basically scalar magnetometer that can be also operated in vector mode using essentially the same setup and varying bias field components.

Classification

1. Magnetic Resonance Magnetometers
   - M_x and M_z Magnetometers
2. Hanle Magnetometers - *Zero-Field Ground State Level Crossing Magnetometers*
   - SERF
3. Light Modulation Magnetometers

Optically Detected Magnetic Resonance Magnetometers

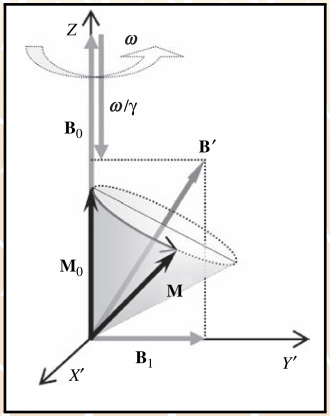

- Bias Field $\gamma B_0 = \omega_0$ along $\hat{z}$
- Oscillating (or rotating) field $\gamma B_1 = \Omega \cos \omega t$

$$\frac{d\mathbf{M}}{dt} = \gamma \mathbf{M} \times \mathbf{B} - \frac{\mathbf{M}}{T_i}$$

Transforming from $(\hat{x}, \hat{y}, \hat{z})$ to rotating frame $(\hat{u}, \hat{v}, \hat{z})$ the stationary solutions are:

$$\mathbf{M}_{\hat{u}} = -M_0 \frac{\Omega T_2}{1 + (\Delta\omega T_2)^2 + \Omega^2 T_1 T_2}$$

$$\mathbf{M}_{\hat{v}} = M_0 \frac{\Delta\omega \Omega T_2^2}{1 + (\Delta\omega T_2)^2 + \Omega^2 T_1 T_2}$$

$$\mathbf{M}_{\hat{z}} = M_0 \frac{1 + (\Delta\omega T_2)^2}{1 + (\Delta\omega T_2)^2 + \Omega^2 T_1 T_2}$$

M_x and M_z magnetometers

There are two main configurations to exploit the magnetic resonance phenomena, M_x and M_z magnetometers.

M_z

The z-component of the spin polarization is detected by a probe beam probe beam directed along the bias field direction. The pump and probe beams carry identical polarization and propagate along the same direction.
The signal is the longitudinal component of magnetic moment.

M_x

Any arrangement in which a polarization component orthogonal to bias field is detected. A 'pure' M_x magnetometer would require two distinct beams. However, it may be realized by a single beam, that reads out simultaneously the x- and z-components of the steady-state polarization.
The signal is the phase of the transverse component of magnetic moment.

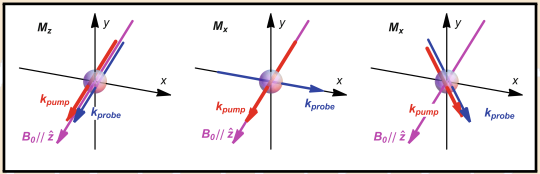

M_z

One may modulate the RF field frequency and observe changes in the absorption of pumping light. The feedback system tunes the mean frequency of the RF field to the frequency of the resonance line center.
For low intensity B_1 the

$$\mathbf{M}_{\hat{z}} = M_0 \frac{1+(\Delta\omega T_2)^2}{1+(\Delta\omega T_2)^2+\Omega^2 T_1 T_2} \underset{\Omega^2 T_1 T_2 << 1}{=} = M_0 \Omega^2 T_1 T_2 \mathcal{L}[\delta\omega T_2]$$

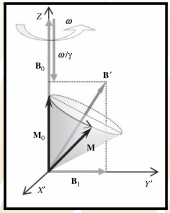

In order to determine the sign and value of the mean detuning $\Delta\omega$ one has to use modulation of ω at low frequency Ω_m ($\Omega_m < 1/T_1, 1/T_2$), accompanied with the synchronous detection of the signal at the same frequency Ω_m.

Disadvantages

- Time response is limited by T_1
- Angular dead zones

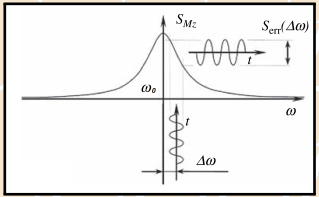

Advantages

- Center of the resonance line position does not depends on the phase of the observed signal
- pumping scheme simplicity, axial symmetry

M_x

A transverse magnetic field B_1 oscillating with frequency ω, which is close to the resonance frequency $\omega_0 = \gamma B_0$.

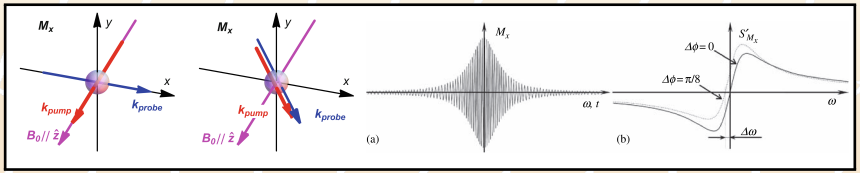

The transverse magnetization is detected using a circularly polarized light beam directed, for example, along the X axis (perpendicular to B).
Then, in a coordinate system with the quantization axis parallel to X , there is a periodic (with frequency ω) change of the absorption coefficient for the transverse light beam. This AC signal can be used for phase locking to the resonance.
In M_x magnetometer the signal acquired reacts instantaneously to magnetic field modulus changes.

M_X - Registration techniques - Self-Oscillating

Light emitted by a Cs lamp is directed at an angle of $45^\circ \pm 15^\circ$ with respect to the measured magnetic field.
The amplified signal is transmitted from the photodetector to the rf coil.
Noise components of the photosignal trigger a priming signal at the Larmor precession frequency in the external magnetic field.
This signal is additionally amplified, phase-shifted, and again transferred to the cell through a feedback loop
The generation frequency is roughly proportional to the strength of the external magnetic field with the proportionality coefficient around 3.5 Hz nT^{-1}.

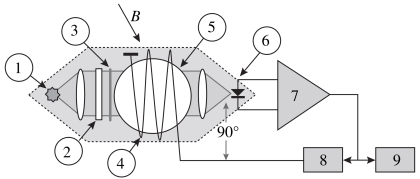

Figure 4.7 The block scheme of a self-oscillating M_X OPQM: 1 spectral lamp, 2 D1 filter, 3 circular polarizer, 4 RF coil, 5 vapor cell, 6 photo detector, 7 amplifier, 8 phase shifter, 9 frequency meter.

M_x - Registration techniques - Non-Self-Oscillating

Has the same optical part of the Self-Oscillating scheme.
Electronic part is "improved" using a PLL (phase locket loop) which allows to select and lock a single resonance resolving the problem of resonance line selection (characteristic of Self-Oscillating scheme).

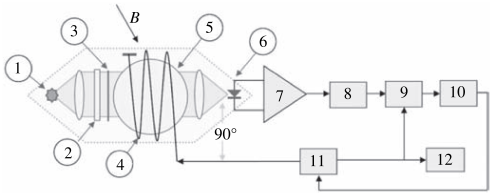

Figure 4.8 PLL M_x magnetometer block-scheme: 1–8 the same as in Fig. 4.7, 9 phase detector, 10 integrating amplifier, 11 voltage-controlled oscillator, 12 frequency meter.

Magnetic Resonance Magnetometers Characteristics and Limitations

M_x

- The signal is proportional to phase of transverse magnetic moment component
- Fast Time response
- Angular dead zones
- Some pumping scheme are simple (Self-Oscillating $15\text{fT}/\sqrt{Hz}$)[3] others are more complicated (Non-Self-Oscillating $1.8\text{fT}/\sqrt{Hz}$)[4]

M_z

- The signal is proportional to the longitudinal component of the magnetic moment
- Time response is limited
- Angular dead zones
- Pumping scheme simplicity, axial symmetry

[3] S. Groeger, G. Bison, J.-L. Schenker, R. Wynands, and A. Weis, "A high-sensitivity laser-pumped mx magnetometer," *The European Physical Journal D - Atomic, Molecular, Optical and Plasma Physics*, vol. 38, pp. 239–247, May 2006

[4] E. Alexandrov, M. Balabas, A. Pasgalev, A. Vershovskii, and N. Yakobson, "Double-resonance atomic magnetometers: From gas discharge to laser pumping," *Laser Physics*, vol. 6, no. 2, pp. 244–251, 1996

An Application

Electromagnetic induction imaging with a radio-frequency atomic magnetometer

Cameron Deans, Luca Marmugi,[a] Sarah Hussain, and Ferruccio Renzoni
Department of Physics and Astronomy, University College London, Gower Street, London WC1E 6BT, United Kingdom

(Received 12 January 2016; accepted 29 February 2016; published online 10 March 2016)

We report on a compact, tunable, and scalable to large arrays imaging device, based on a radio-frequency optically pumped atomic magnetometer operating in magnetic induction tomography modality. Imaging of conductive objects is performed at room temperature, in an unshielded environment and without background subtraction. Conductivity maps of target objects exhibit not only excellent performance in terms of shape reconstruction but also demonstrate detection of sub-millimetric cracks and penetration of conductive barriers. The results presented here demonstrate the potential of a future generation of imaging instruments, which combine magnetic induction tomography and the unmatched performance of atomic magnetometers.
[http://dx.doi.org/10.1063/1.4943659]

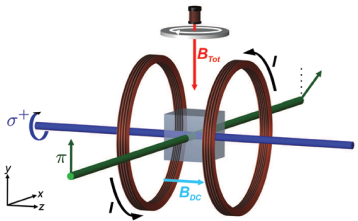

$$\mathbf{B_{Tot}} = \mathbf{B_{RF}} + \mathbf{B_{EC}}$$

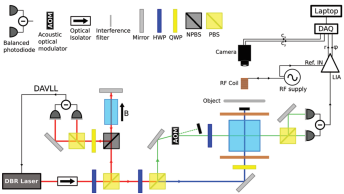

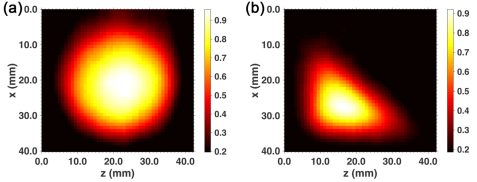

FIG. 2. Electromagnetic induction imaging with a RF OAM: normalized conductivity maps of Al objects at 1 kHz. (a) R map of an Al disk, diameter 37 mm (2 mm thick). $C \approx 3.5$, as defined in Eq. (1). (b) ϕ map of a 31 mm × 38 mm × 50 mm Al triangle (3 mm thick). $C \approx 3.9$. Maximum phase change is $\Delta\phi_{max} = 41.3°$, the color bar maps an interval $\Delta\phi_{col} = 38.4°$.

Hanle Magnetometers

The 1920s W. Hanle observed that the degree of polarization of the resonance fluorescence changes when the medium is exposed to a static magnetic field.
The effect manifests itself as a resonance structure, centered at $B = 0$.
The effect is known as zero-field level crossing, or just the Hanle effect (HE).

SERF

Working Principle

Ideal operation in the SERF regime, the magnetic field must be exactly zero. Narrow atomic resonance. Sometimes a finite bias field is applied.

If a SERF magnetometer is applied to magnetoencephalography (MEG), it might need to cover a 100 Hz frequency range of the brain neural activity spectrum, and bias-field tuning can help to extend sensitive operation over this range as an alternative to broadening the atomic magnetometer resonance. Thus it is interesting for practical applications to cover a range of atomic magnetometer resonance parameters where the SE contribution to relaxation is not negligible

SERF

Working Principle

Ideal operation in the SERF regime, the magnetic field must be exactly zero. Narrow atomic resonance. Sometimes a finite bias field is applied.

$$\frac{d\rho}{dt} = A_{hf}\frac{[\boldsymbol{I}\cdot\boldsymbol{S},\rho]}{i\hbar} + \mu_B g_S \frac{[\boldsymbol{B}\cdot\boldsymbol{S},\rho]}{i\hbar} + \frac{\phi(1+4\langle\boldsymbol{S}\rangle\cdot\boldsymbol{S})-\rho}{T_{SE}} + \frac{\phi-\rho}{T_{SD}} + R[\phi(1+2\boldsymbol{s}\cdot\boldsymbol{S})-\rho] + D\nabla^2\rho$$

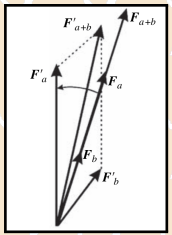

- F_a and F_b are aligned
- $B_\perp$, during the time between spin coliisions $F_a \rightarrow F'_a$, and $F_b \rightarrow F'_b$
- Spin collision $F'_a + F'_b \rightarrow F'_{a+b}$
- Reduction of the total angular momentum by $F_{a+b} - F'_{a+b}$
- Only the transverse component of the spin and hence only transverse polarization is changed. $\rightarrow$ SE collisions contribute to T_2 but not T_1
- T_2 Depends quadratically on B
- If polarization is high a $F_a >> F_b$, SE broadenign is reduced

SERF

Working Principle

Ideal operation in the SERF regime, the magnetic field must be exactly zero. Narrow atomic resonance. Sometimes a finite bias field is applied.

$$\frac{d\rho}{dt} = A_{hf}\frac{[\boldsymbol{I}\cdot\boldsymbol{S},\rho]}{i\hbar} + \mu_B g_S \frac{[\boldsymbol{B}\cdot\boldsymbol{S},\rho]}{i\hbar} + \frac{\phi(1+4\langle\boldsymbol{S}\rangle\cdot\boldsymbol{S})-\rho}{T_{SE}} + \frac{\phi-\rho}{T_{SD}} + R[\phi(1+2\boldsymbol{s}\cdot\boldsymbol{S})-\rho] + D\nabla^2\rho$$

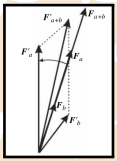

Foundamental Sensitivity

Superior sensitivity due to dramatic reduction in bandwidth when the effect of SE collisions on $T2$ relaxation is turned off.

Experimental Realization

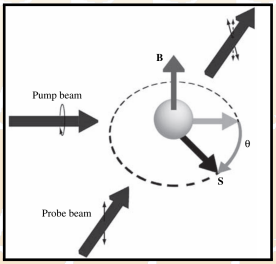

Figure: Typical arrangement of a SERF magnetometer, with a circularly polarized pump beam tuned to the D1 line and a linearly polarized probe beam tuned slightly off the D1 line

SERF Characteristics and Limitations

- Larmor frequency drift ($\frac{4}{11}\omega$ for Cs)
- Narrow resonance
- High sensitivity
- Very low bandwidth
- Operates in very low and homogeneous magnetic field

Light Modulation Magnetometer - Working Principle

Two Beams - Circular-polarized pump light

Bell and Bloom realized an alternative method for optical magnetometry modulating the light used for optical pumping at a frequency resonant with the Larmor precession of atomic spins (or a subharmonic)[5].

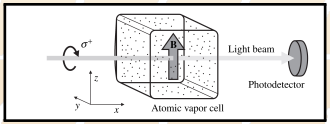

In a Bell–Bloom optical magnetometer, circularly polarized light resonant with an atomic transition propagates through an atomic vapor along a direction transverse to a magnetic field B. Atomic spins immersed in B precess at the Larmor frequency Ω_L, and when the light intensity is modulated at $\Omega_m = \Omega_L$, a resonance in the transmitted light intensity is observed.
In analogy with a driven harmonic oscillator, in a magnetic field B atomic spins precess at a natural frequency equal to Ω_L and the light acts as a driving force oscillating at the modulation frequency Ω_m.

[5] W. E. Bell and A. L. Bloom, "Optically driven spin precession," *Phys. Rev. Lett.*, vol. 6, pp. 280–281, Mar 1961

Light Modulation Magnetometer

- Anything that changes the light–atom interaction probability can be used as a source of modulation to generate a magnetic resonance signal, and so one can construct opticalmagnetometers based on amplitude, frequency, or polarization modulation of the light.

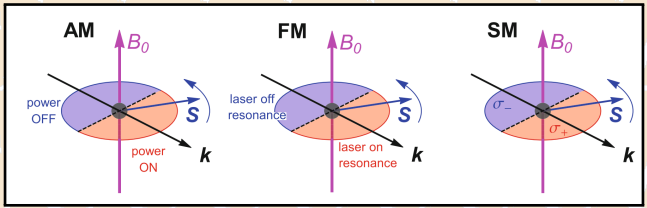

Apparatus scheme

A Multichannel Optical Magnetometer Operating in Unshielded Environment

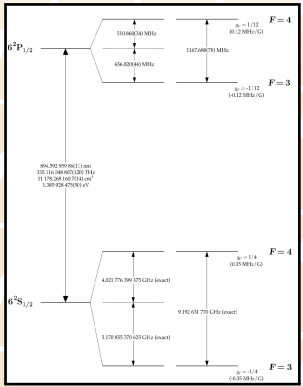

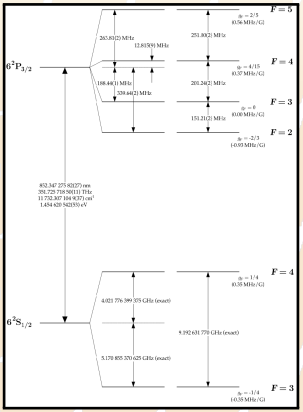

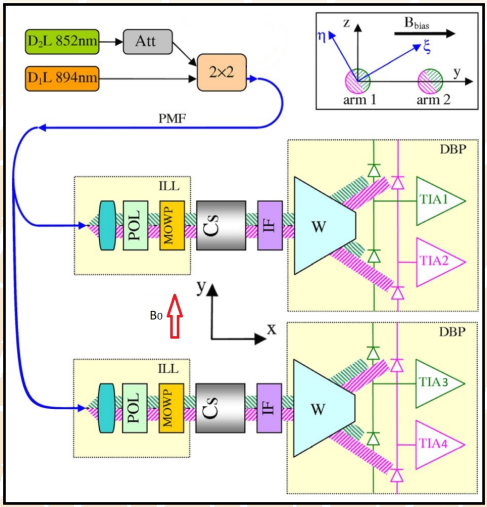

Light Modulation

Pump laser

- Single mode
- DFB
- PigTailed

Probe laser

- Single mode
- Fabry Perot
- PigTailed

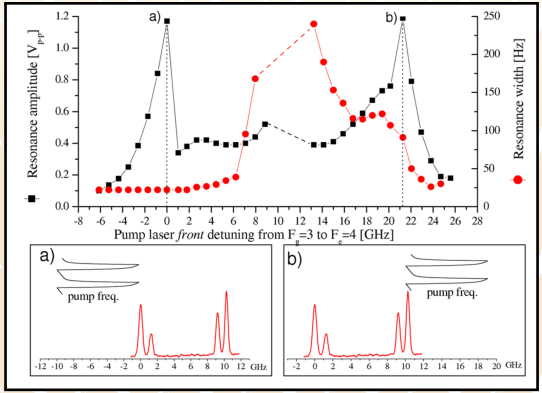

G. Bevilacqua, V. Biancalana, P. Chessa, and Y. Dancheva, "Multichannel optical atomic magnetometer operating in unshielded environment," *Applied Physics B*, vol. 122, p. 103, Apr 2016

The Magnetometer

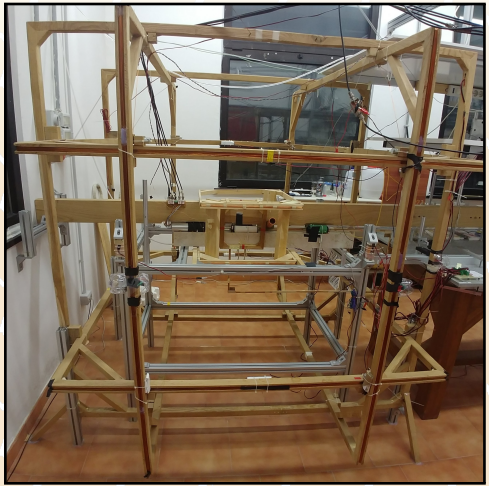

Polarimetric Signal Phase

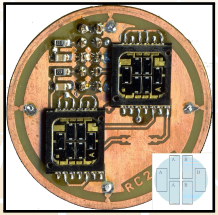

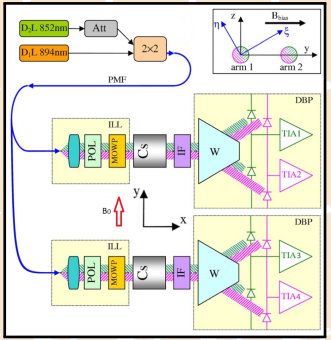

$$\vec{B}(t) = [B_{bias} + \delta B(t)]\hat{y}$$

$$\omega_L = \gamma B_{bias} \text{ and } \omega_1 = \gamma \delta B(t)$$

Polarimetric Signal Phase

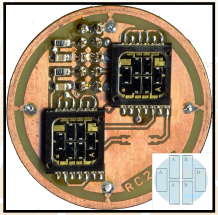

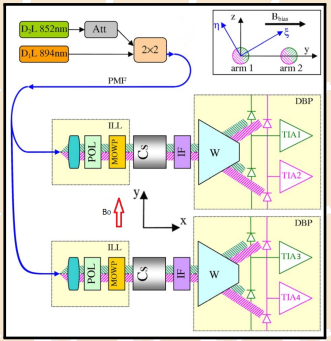

$$\vec{B}(t) = [B_{bias} + \delta B(t)]\hat{y}$$

$$\omega_L = \gamma B_{bias} \text{ and } \omega_1 = \gamma \delta B(t)$$

Bloch Equations

$$\dot{M}_x = -\Gamma M_x + (\omega_L + \omega_1)M_z + f(t)$$

$$\dot{M}_y = -\Gamma M_y$$

$$\dot{M}_z = -\Gamma M_z - (\omega_L + \omega_1)M_x$$

$$M_+ = M_x + iM_z \quad \rightarrow \quad \dot{M}_+ = [-\Gamma - i(\omega_L + \omega_1)]M_+ f(t)$$

Polarimetric Signal Phase

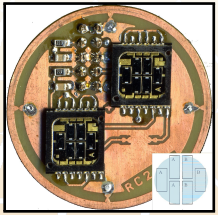

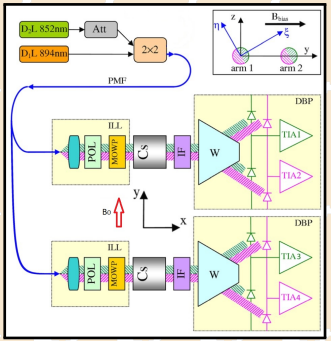

$$\vec{B}(t) = [B_{bias} + \delta B(t)]\hat{y}$$

$$\omega_L = \gamma B_{bias} \text{ and } \omega_1 = \gamma \delta B(t)$$

Bloch Equations

$$\dot{M}_x = -\Gamma M_x + (\omega_L + \omega_1)M_z + f(t)$$

$$\dot{M}_y = -\Gamma M_y$$

$$\dot{M}_z = -\Gamma M_z - (\omega_L + \omega_1)M_x$$

$$M_+ = M_x + iM_z \quad \rightarrow \quad \dot{M}_+ = [-\Gamma - i(\omega_L + \omega_1)]M_+ f(t)$$

Solution is:

$$M = \cos(\omega_t + \phi(t))$$

Where $\omega_1 = \gamma \delta B(t)$ is related to $\phi(t)$ through:

$$\omega_1 = -\Gamma\phi - \dot{\phi} - \Delta$$

$$\delta B = \frac{1}{\gamma}[-\dot{\phi} - \Gamma\phi - \Delta]$$

The signal

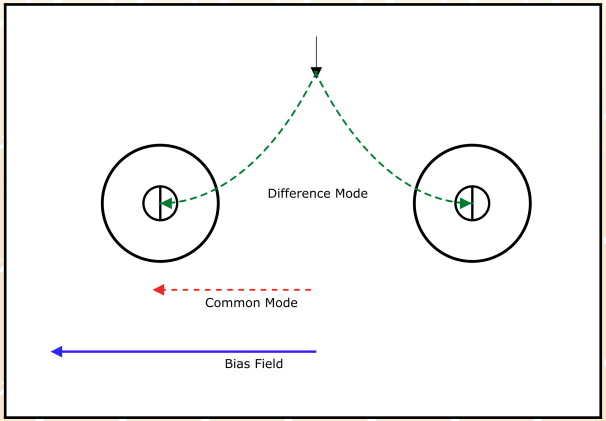

- Compensation System
- NMR
- MRI

The compensation system(1)

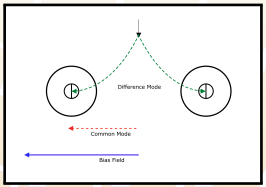

The Idea

$$\dot{M}_+ = [-\Gamma - i(\omega_L + \omega_1)]M_+ f(t)$$

$$\dot{M}_+ = [-\Gamma - i(\omega_L + \omega_{1,CM} + \omega_{1,DM})]M_+ f(t)$$

$$\delta B = \frac{1}{\gamma}[-\dot{\phi} - \Gamma\phi - \Delta]$$

$$\dot{M}_+ = [-\Gamma - i(\omega_L + \omega_1 - \delta B_{CM})]M_+ f(t)$$

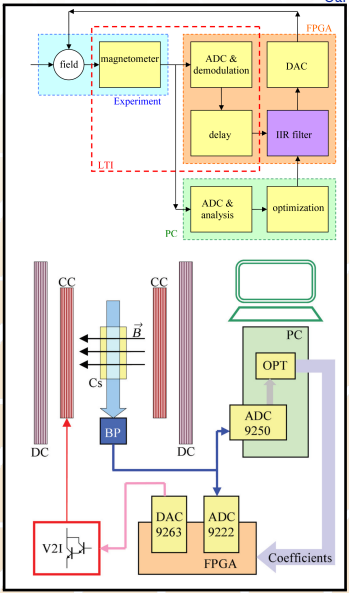

G. Bevilacqua, V. Biancalana, Y. Dancheva, and A. Vigilante, "Self-adaptive loop for external-disturbance reduction in a differential measurement setup," *Phys. Rev. Applied*, vol. 11, p. 014029, Jan 2019

The compensation system(2)

The implementation

- Measure $M = \cos(\omega_t + \phi(t))$
- Discrete signal M_i
- Demodulation $\phi_i(t)$
- Filter (IIR) $B_n = \sum_{i=n-r}^{n} c_i M_i + \sum_{i=n-r}^{n-1} b_i B_i$
- Amplification of signal
- Coils

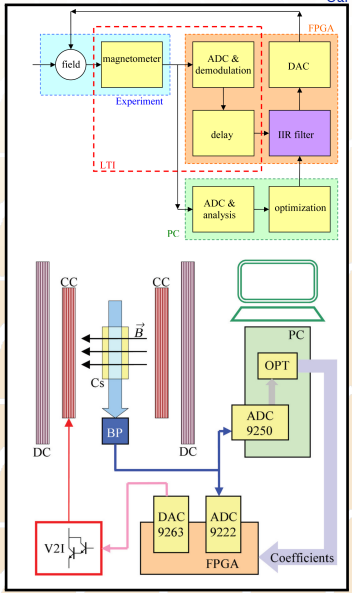

G. Bevilacqua, V. Biancalana, Y. Dancheva, and A. Vigilante, "Self-adaptive loop for external-disturbance reduction in a differential measurement setup," *Phys. Rev. Applied*, vol. 11, p. 014029, Jan 2019

The optimization system

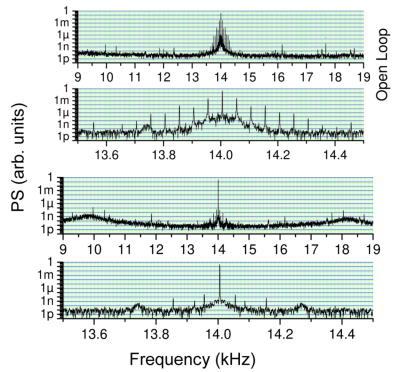

FIG. 5. The power spectra, in a wide (upper plot) and a narrow (lower plot) frequency range, of the polarimetric signal of a single magnetometer channel in open loop (a) and in closed loop with an FIR loop filter designed according to the magnetometer frequency response (b).

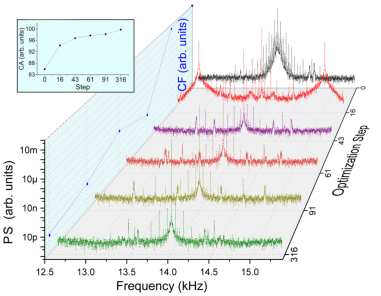

FIG. 6. A sample of a few significative steps in the optimization procedure. Starting from the uncompensated case (step 0), a progressive improvement of the polarimetric signal spectra is achieved. The improvement appears in the power spectrum (PS) and consists in the fact that both the pedestal and the peaks around the carrier frequency are lower than in the uncompensated case. The CF reduction is represented in the blue plot on the left vertical plane.

LowField NMR

Contents lists available at ScienceDirect

Journal of Magnetic Resonance

journal homepage: www.elsevier.com/locate/jmr

Microtesla NMR *J*-coupling spectroscopy with an unshielded atomic magnetometer

Giuseppe Bevilacqua [a], Valerio Biancalana [a,*], Andrei Ben-Amar Baranga [b], Yordanka Dancheva [c], Claudio Rossi [d]

[a] DIISM, University of Siena, Italy
[b] Dep. of Electr. and Computer Engin., Ben-Gurion University of the Negev, Israel
[c] DSFTA, University of Siena, Italy
[d] DBCF, University of Siena, Italy

THE JOURNAL OF PHYSICAL CHEMISTRY Letters

Letter

Cite This: J. Phys. Chem. Lett. 2017, 8, 6176−6179

pubs.acs.org/JPCL

Simultaneous Detection of H and D NMR Signals in a Micro-Tesla Field

Giuseppe Bevilacqua,[†] Valerio Biancalana,*[,†] Yordanka Dancheva,[‡] Antonio Vigilante,[‡] Alessandro Donati,[§] and Claudio Rossi[§]

[†]Department of Information Engineering and Mathematics (DIISM), University of Siena, 53100 Siena, Italy
[‡]Department of Physical Sciences, Earth and Environment (DSFTA), University of Siena, 53100 Siena, Italy
[§]Department of Biotechnology, Chemistry and Pharmacy (DBCF), University of Siena, 53100 Siena, Italy

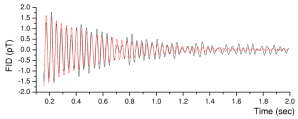

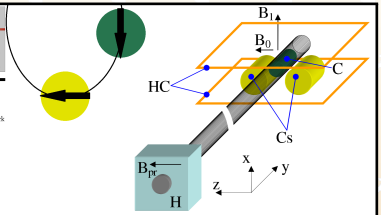

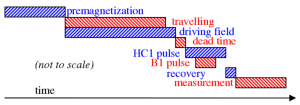

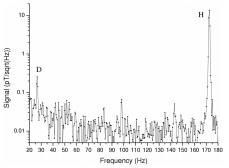

Dressing (1)

PHYSICAL REVIEW A **85**, 042510 (2012)

Larmor frequency dressing by a nonharmonic transverse magnetic field

G. Bevilacqua, V. Biancalana, Y. Dancheva, and L. Moi
CNISM, CSC and Dipartimento di Fisica, Università di Siena, via Roma 56, 53100 Siena, Italy
(Received 7 December 2011; published 9 April 2012)

We present a theoretical and experimental study of spin precession in the presence of both a static and an orthogonal oscillating magnetic field, which is nonresonant, not harmonically related to the Larmor precession, and of arbitrary strength. Due to the intrinsic nonlinearity of the system, previous models that account only for the simple sinusoidal case cannot be applied. We suggest an alternative approach and develop a model that closely agrees with experimental data produced by an optical-pumping atomic magnetometer. We demonstrate that an appropriately designed nonharmonic field makes it possible to extract a linear response to a weak dc transverse field, despite the scalar nature of the magnetometer, which normally causes a much weaker, second-order response.

DOI: 10.1103/PhysRevA.85.042510 PACS number(s): 32.30.Dx, 32.10.Dk, 32.80.Xx

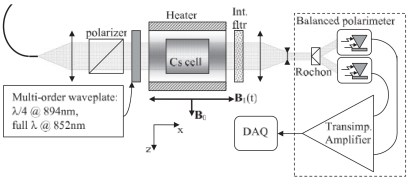

$$(B_x \cos(\omega t), 0, B_z)$$

$$\xi \equiv \Omega_x/\omega\,;\ \Omega_z/\omega \ll 1$$

$$\Omega_L = \Omega_z |J_0(\xi)|$$

Dressing (2)

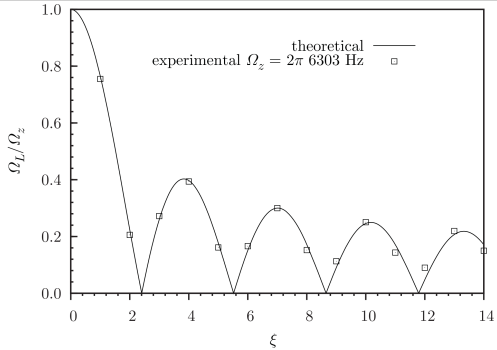

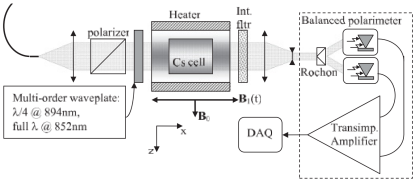

$$(B_x \cos(\omega t), 0, B_z)$$

$$\xi \equiv \Omega_x/\omega\,;\ \Omega_z/\omega \ll 1$$

$$\Omega_L = \Omega_z\,|J_0(\xi)|$$

Inhomogeneous Dressing For Imaging

Restoring Narrow Linewidth to a Gradient-Broadened Magnetic Resonance by Inhomogeneous Dressing

Giuseppe Bevilacqua,[1] Valerio Biancalana,[1,*] Yordanka Dancheva,[2] and Antonio Vigilante[2]

[1] *Department of Information Engineering and Mathematics—DIISM, University of Siena, Via Roma 56, 53100 Siena, Italy*

[2] *Department of Physical Sciences, Earth and Environment—DSFTA, University of Siena, Via Roma 56, 53100 Siena, Italy*

(Received 4 July 2018; revised manuscript received 11 December 2018; published 20 February 2019)

We study the possibility of counteracting the line broadening of atomic magnetic resonances due to inhomogeneities of the static magnetic field by means of spatially dependent magnetic dressing, driven by an alternating field that oscillates much faster than the Larmor precession frequency. We demonstrate that an intrinsic resonance linewidth of 25 Hz that has been broadened up to hundreds of hertz by a magnetic field gradient can be recovered by the application of an appropriate inhomogeneous dressing field. The findings of our experiments may have immediate and important implications, because they enable the use of atomic magnetometers as robust, high-sensitivity sensors to detect *in situ* the signal from ultralow-field NMR-imaging setups.

DOI: 10.1103/PhysRevApplied.11.024049

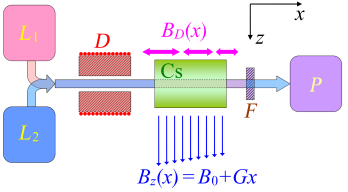

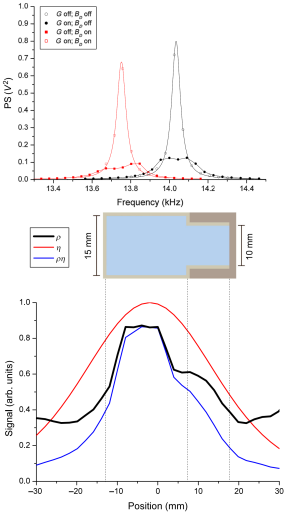

Inhomogeneous Dressing For Imaging

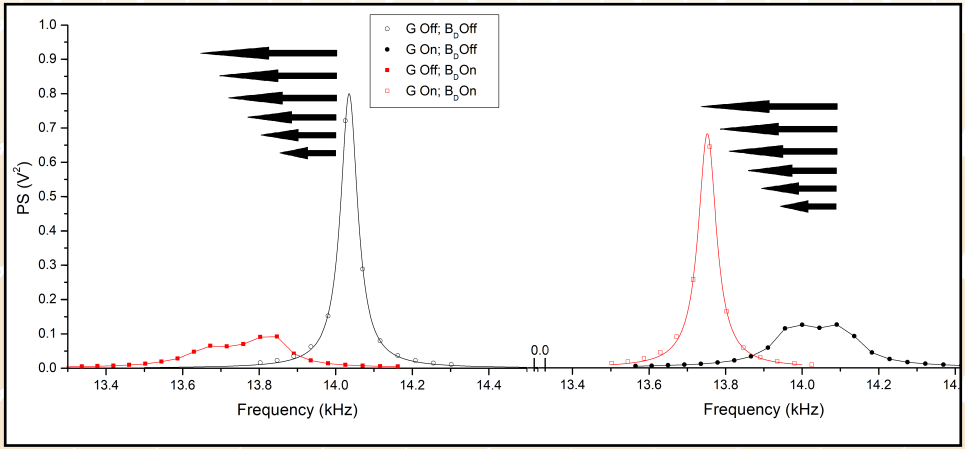

Inhomogeneous Dressing For Imaging

Restoring Narrow Linewidth to a Gradient-Broadened Magnetic Resonance by Inhomogeneous Dressing

Giuseppe Bevilacqua,[1] Valerio Biancalana,[1,*] Yordanka Dancheva,[2] and Antonio Vigilante[2]

[1] *Department of Information Engineering and Mathematics—DIISM, University of Siena, Via Roma 56, 53100 Siena, Italy*

[2] *Department of Physical Sciences, Earth and Environment—DSFTA, University of Siena, Via Roma 56, 53100 Siena, Italy*

(Received 4 July 2018; revised manuscript received 11 December 2018; published 20 February 2019)

We study the possibility of counteracting the line broadening of atomic magnetic resonances due to inhomogeneities of the static magnetic field by means of spatially dependent magnetic dressing, driven by an alternating field that oscillates much faster than the Larmor precession frequency. We demonstrate that an intrinsic resonance linewidth of 25 Hz that has been broadened up to hundreds of hertz by a magnetic field gradient can be recovered by the application of an appropriate inhomogeneous dressing field. The findings of our experiments may have immediate and important implications, because they enable the use of atomic magnetometers as robust, high-sensitivity sensors to detect *in situ* the signal from ultralow-field NMR-imaging setups.

DOI: 10.1103/PhysRevApplied.11.024049

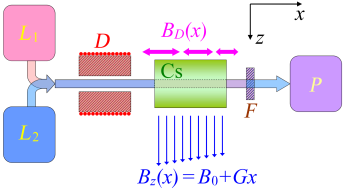

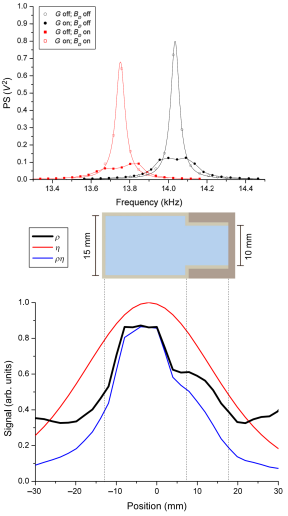

Thank You For Your Attention

I. Fescenko and A. Weis, "Imaging magnetic scalar potentials by laser-induced fluorescence from bright and dark atoms," *Journal of Physics D: Applied Physics*, vol. 47, p. 235001, may 2014

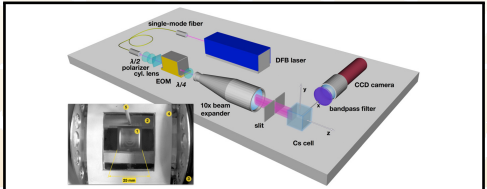

Figure 1. Schematic layout of the apparatus, not including magnetic field coils. The photograph shows the central part of the set-up, as seen by the CCD camera. One distinguishes: the cubic vapour cell (1) with ring-structured fluorescence produced by the 1 WH field configuration, one of the support structures for the rf coils (2), the coils producing the quadrupole field (3), a support structure for the eight wires of the 8W-configuration (4), and the protruding 'wire' of the 1 WH field configuration.

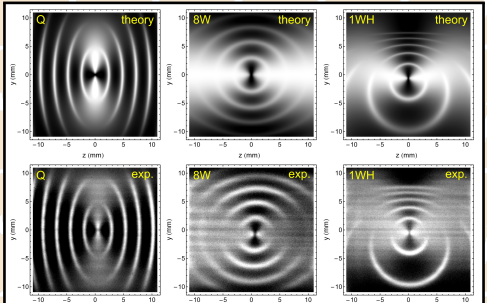

Fundamental Sensitivity(2)

There is also a contribution to optical-magnetometer noise from the quantum uncertainty of measurements of light properties (photon shot noise). Optical detection of atomic spin precession is usually performed by measuring either the intensity or polarization of light transmitted through the atomic sample.
If, for example, atomic spin precession is detected by measuring optical rotation of the plane of transmitted light polarization, the photon-shot-noise-limited sensitivity to the optical rotation angle ϕ is

$$\delta\phi \approx \frac{1}{2}\sqrt{\frac{1}{\Phi\tau}}$$

where Φ is the probed photon flux (photons/s) detected after the atomic sample and $\delta\phi$ is measured in $rad/\sqrt{Hz}$. In optimal operation, the contribution of photon shot noise to overall magnetometric noise does not exceed the contribution from atomic spin-projection noise.

Optical Magnetometry. Cambridge University Press, 2013

Light Modulation Magnetometer - Working Principle

Difference over setups consist on beams polarization, number, geometrical arrangement and kind of modulation.

Single Beam - Linearly-polarized pump light

- DC NMOR - The linear polarized pump propagates through an atomic medium along the direction of an applied magnetic field. The magnetic field splits Zeeman sublevels causing phase oscillations proportional to the difference of energy levels. These signals allow for a magnetic-field sensitivity of 10^{-15} T/$\sqrt{Hz}$ detectable in a dynamic field range of roughly 10^{10} T.[6]
- FM NMOR - A frequency-modulated light beam is employed for optical pumping and detection of NMOR resonances[7].
- AM NMOR - Another approach to optical magnetometry is the measurement of NMOR resonances with amplitude-modulated light.

In both AM and FM configuration the possibility to modify the modulation frequency makes possible to detect stronger magnetic fields and extend the dynamic range to the fields exceeding the Earth's magnetic field. Note that at stronger fields, the high-field NMOR signal deteriorates due to the nonlinearity (Zeeman).

[6] D. Budker, V. Yashchuk, and M. Zolotorev, "Nonlinear magneto-optic effects with ultranarrow widths," *Phys. Rev. Lett.*, vol. 81, pp. 5788–5791, Dec 1998

[7] D. Budker, D. F. Kimball, V. V. Yashchuk, and M. Zolotorev, "Nonlinear magneto-optical rotation with frequency-modulated light," *Phys. Rev. A*, vol. 65, May 2002